arXiv:cond-mat/0202308v1 [cond-mat.mtrl-sci] 19 Feb 2002

All-electron GW calculation based on the LAPW method: application to wurtzite ZnO

Manabu Usuda and Noriaki Hamada
Department of Physics, Faculty of Science and Technology,
Tokyo University of Science,
2641 Yamazaki, Noda, Chiba 278-8510, Japan

Takao Kotani
Department of Physics, Osaka University, 1-16 Machikaneyama, Toyonaka 560, Japan

Mark van Schilfgaarde
Sandia National Laboratory, Livermore, CA U.S.A.

(Dated: February 1, 2008)

We present a new, all-electron implementation of the GW approximation and apply it to wurtzite ZnO. Eigenfunctions computed in the local-density approximation (LDA) by the full-potential linearized augmented-plane-wave (LAPW) or the linearized muffin-tin-orbital (LMTO) method supply the input for generating the Green function G and the screened Coulomb interaction W. A mixed basis is used for the expansion of W, consisting of plane waves in the interstitial region and augmented-wavefunction products in the augmentation-sphere regions. The frequency-dependence of the dielectric function is computed within the random-phase approximation (RPA), without a plasmon-pole approximation. The Zn $3d$ orbitals are treated as valence states within the LDA; both core and valence states are included in the self-energy calculation. The calculated bandgap is smaller than experiment by ∼1 eV, in contrast to previously reported GW results. Self-energy corrections are orbital-dependent, and push down the deep O $2s$ and Zn $3d$ levels by ∼1 eV relative to the LDA. The d level shifts closer to experiment but the size of shift is underestimated, suggesting that the RPA overscreens localized states.

I. INTRODUCTION

Density-functional theory (DFT) provides a foundation for modern electronic-structure calculations, and the local-density approximation (LDA) is an efficient way to calculate the ground-state properties of material. However, the LDA eigenvalues should not necessarily identified with the quasiparticle (QP) energies, although eigenvalue differences are often used to describe the excited state. Time-dependent DFT can in principle describe the excited state, but a good approximation for the time-dependent exchange-correlation kernel is not known. The GW approximation (GWA) of Hedin [1] provides a practical method to calculate the QP energy. Hybertsen and Louie presented the first GW calculation for real materials in 1986 [2]. They employed eigenfunctions given by the LDA as input, using additionally a pseudopotential approximation.

Several methods have since been developed within various band-structure-calculation schemes [3]. Calculated QP energies typically agree well with experiment, for many kinds of materials. However, various kinds of approximations in addition to the GW approximation itself are usually employed, whose adequacy has not been well tested. Here we present a method that makes minimal approximations in addition to the GW and random-phase approximations. We start with the LDA eigenfunctions generated by the full-potential linearized augmented-plane-wave (LAPW) [4] or a variant of the full-potential linearized muffin-tin-orbital (LMTO) method [5, 6], where in either case eigenfunctions are expanded in atomic-like local functions in the muffin-tin (MT) sphere regions, and in plane waves in the interstitial region. In order to treat the localized electrons accurately, the Coulomb interaction v and the screened Coulomb interaction W are expanded with a newly-developed mixed basis that consists of two kinds of basis functions. One is the product-basis function developed by Aryasetiawan and Gunnarsson [7], which is constructed from the products of the local functions in the MT-sphere regions. The other is the interstitial plane wave (IPW) that takes zero in the MT-sphere regions and equals to the usual plane wave in the interstitial region. With the mixed basis, we can treat localized electrons, even core electrons, on the same footing as the other extended electrons. The mixed basis is by construction essentially a complete basis for the expansion of W; therefore, for given eigenfunctions as input, our method can produce reasonably well converged QP energies rather more efficiently than a method that expands W in plane waves alone.

The LMTO method employs smooth Hankel functions as envelope functions [6], which are smoother and more accurate than the ordinary Hankel functions customary to the LMTO method. About 100 envelope functions were employed in this calculation. To check convergence, empty sphere was added to some of the calculations, mainly to enlarge the basis set. However, little difference was found whether the empty sphere was added or not.

We apply this approach to wurtzite-type ZnO, whose valence bands consist of extended O $2p$ and Zn $4s$ orbitals, and rather localized Zn $3d$ and O $2s$ orbitals. ZnO is important for optical device technology since the material is optically transparent and can be doped with both electrons and holes [8]. Compared with most other II-VI and III-V compounds such as ZnS, GaN, etc., the position of the cation d levels are rather high, and relatively close to the anion p-derived valence band maximum (VBM). The effect of the Zn $3d$ state is not negligible for the various properties. For example, the $3d$ state couples to the VBM and pushes it upward, reducing the bandgap.

This paper is organized as follows. Section II briefly describes the method. In Sec. III, we show LDA and *GW* results for ZnO, and compare them to experimental data and previously reported *GW* results. A summary is given in Sec. IV.

II. OVERVIEW OF THE *GW* CALCULATION

The brief procedure of our *GW* calculation is presented here; it will be described in more detail elsewhere [9]. In the Green's-function approach, the QP energy $E_{\mathbf{k}n}$ and wavefunction $f_{\mathbf{k}n}(\mathbf{r})$ of a many-electron system are given as the solution of the equation

$$\begin{aligned}[E_{\mathbf{k}n} - T - V_{\mathrm{H}}(\mathbf{r})]f_{\mathbf{k}n}(\mathbf{r}) \\ - \int \Sigma(\mathbf{r},\mathbf{r}',E_{\mathbf{k}n})f_{\mathbf{k}n}(\mathbf{r}')d^3r' = 0, \end{aligned} \tag{1}$$

where T is the kinetic-energy operator, V_{H} is the Hartree potential plus the electrostatic potential from nuclei, and Σ is the self-energy. In the *GW* approximation, the self-energy is written as

$$\Sigma(\mathbf{r},\mathbf{r}',\omega) = i\int_{-\infty}^{\infty}\frac{d\omega'}{2\pi}e^{i\omega'\delta}G(\mathbf{r},\mathbf{r}',\omega+\omega')W(\mathbf{r},\mathbf{r}',\omega'). \tag{2}$$

It is convenient to divide Σ into $\Sigma = \Sigma_{\mathrm{x}} + \Sigma_{\mathrm{c}}$, with $\Sigma_{\mathrm{x}} = iGv$ the bare exchange term, and $\Sigma_{\mathrm{c}} = iGW_{\mathrm{c}}$ the correlation term. Here $W_{\mathrm{c}} \equiv W - v$.

We take a perturbative approach to find $E_{\mathbf{k}n}$. First, we solve the Kohn-Sham (KS) equation,

$$[\epsilon_{\mathbf{k}n} - T - V_{\mathrm{H}}(\mathbf{r}) - V_{\mathrm{xc}}^{\mathrm{LDA}}(\mathbf{r})]\psi_{\mathbf{k}n}(\mathbf{r}) = 0, \tag{3}$$

where $V_{\mathrm{xc}}^{\mathrm{LDA}}(\mathbf{r})$ is the exchange-correlation potential in the LDA. We assume that $\Sigma - V_{\mathrm{xc}}^{\mathrm{LDA}}$ is small enough to be treated a first-order quantity. Expanding $\Sigma(E_{\mathbf{k}n})$ around $\epsilon_{\mathbf{k}n}$, we obtain to first order

$$E_{\mathbf{k}n} \simeq \epsilon_{\mathbf{k}n} + Z_{\mathbf{k}n}[\langle\psi_{\mathbf{k}n}|\Sigma(\epsilon_{\mathbf{k}n})|\psi_{\mathbf{k}n}\rangle - \langle\psi_{\mathbf{k}n}|V_{\mathrm{xc}}^{\mathrm{LDA}}|\psi_{\mathbf{k}n}\rangle], \tag{4}$$

where $Z_{\mathbf{k}n}$ is the renormalization factor defined by

$$Z_{\mathbf{k}n} = [1 - \langle\psi_{\mathbf{k}n}|(\partial\Sigma/\partial\omega)|_{\omega=\epsilon_{\mathbf{k}n}}|\psi_{\mathbf{k}n}\rangle]^{-1}. \tag{5}$$

We also estimate the first-order energy in the Hartree-Fock approximation (HFA) through

$$E_{\mathbf{k}n}^{\mathrm{HFA}} = \epsilon_{\mathbf{k}n} + \langle\psi_{\mathbf{k}n}|\Sigma_{\mathrm{x}}|\psi_{\mathbf{k}n}\rangle - \langle\psi_{\mathbf{k}n}|V_{\mathrm{xc}}^{\mathrm{LDA}}|\psi_{\mathbf{k}n}\rangle, \tag{6}$$

although the KS wavefunction may be different from the HFA one, and, therefore, $E_{\mathbf{k}n}^{\mathrm{HFA}}$ is not the true self-consistent HFA value.

In the augmented-waves methods, space is divided into the MT-sphere regions and the interstitial region. In both LAPW and the present LMTO method, the KS wavefunction is expanded as

$$\psi_{\mathbf{k}n}(\mathbf{r}) = \sum_{lm}\sum_{\beta=1,2}A_{alm\beta}(\mathbf{r})\alpha_{alm\beta}^{\mathbf{k}n} + \sum_{\mathbf{G}}P_{\mathbf{G}}^{\mathbf{k}}(\mathbf{r})z_n^{\mathbf{k}+\mathbf{G}} \tag{7}$$

where the atomic-like local function $A_{alm\beta}(\mathbf{r})$ is defined by

$$A_{alm\beta}(\mathbf{r}) = \begin{cases}\phi_{al\beta}(r)Y_{lm}(\hat{\mathbf{r}}) & \text{in the } a\text{-atom MT-sphere} \\ 0 & \text{otherwise}\end{cases} \tag{8}$$

with orthogonal radial wavefunctions $\phi_{al\beta}(r)$ ($\beta = 1$ or 2), and spherical harmonics $Y_{lm}(\hat{\mathbf{r}})$. The IPW $P_{\mathbf{G}}^{\mathbf{k}}(\mathbf{r})$ is defined by

$$P_{\mathbf{G}}^{\mathbf{k}}(\mathbf{r}) = \begin{cases}0 & \text{in the MT-sphere regions} \\ e^{i(\mathbf{k}+\mathbf{G})\cdot\mathbf{r}} & \text{in the interstitial region .}\end{cases} \tag{9}$$

The interactions, v and W, are well expressed by the product of two KS eigenfunctions in our perturbative treatment. The product $\psi_{\mathbf{k}_1n_1}(\mathbf{r})\psi_{\mathbf{k}_2n_2}(\mathbf{r})$ is expanded by the product of two local functions, $A_{al_1m_1\beta_1}(\mathbf{r})A_{al_2m_2\beta_2}(\mathbf{r})$, in the MT-sphere regions, and by the product of two plane waves, $P_{\mathbf{G}_1}^{\mathbf{k}_1}(\mathbf{r})P_{\mathbf{G}_2}^{\mathbf{k}_2}(\mathbf{r})$, in the interstitial region. Following Aryasetiawan and Gunnarsson [7] the complete set of product functions is reduced by eliminating nearly linearly dependent ones. Taking the Bloch sum of the product functions, we finally obtain the product-basis function expressed as $B_{a\mu}^{\mathbf{k}}(\mathbf{r})$ in the a-atom MT-sphere region. The product of IPW's is also IPW in the interstitial region: $P_{\mathbf{G}_1}^{\mathbf{k}_1}(\mathbf{r})P_{\mathbf{G}_2}^{\mathbf{k}_2}(\mathbf{r}) = P_{\mathbf{G}_1+\mathbf{G}_2}^{\mathbf{k}_1+\mathbf{k}_2}(\mathbf{r})$. Thus, we obtain a mixed basis $\{M_i^{\mathbf{k}}(\mathbf{r})\} \equiv \{B_{a\mu}^{\mathbf{k}}(\mathbf{r}), P_{\mathbf{G}}^{\mathbf{k}}(\mathbf{r})\}$ which is suitable for expansions of v and W. The index i specifies a member of the basis and runs through $\mathbf{G}$ and $a\mu$.

Because of the nonorthogonality of IPW's, the overlap integral of the mixed-basis functions,

$$S_{ij} \equiv \langle M_i^{\mathbf{k}}|M_j^{\mathbf{k}}\rangle\ ,$$

is nonvanishing for $i \neq j$. We therefore define the dual-basis function:

$$\tilde{M}_i^{\mathbf{k}}(\mathbf{r}) \equiv \sum_{i'}M_{i'}^{\mathbf{k}}(\mathbf{r})S_{i'i}^{-1}\ . \tag{10}$$

The Coulomb interaction v is expanded as

$$\begin{aligned} v(\mathbf{r},\mathbf{r}') &= \sum_{\mathbf{k}}^{\mathrm{BZ}}\sum_{ij}\tilde{M}_i^{\mathbf{k}}(\mathbf{r})v_{ij}(\mathbf{k})(\tilde{M}_j^{\mathbf{k}}(\mathbf{r}'))^* \\ v_{ij}(\mathbf{k}) &= \langle M_i^{\mathbf{k}}|v|M_j^{\mathbf{k}}\rangle\ . \end{aligned} \tag{11}$$

The Coulomb matrix $v_{ij}(\mathbf{k})$ can be calculated by using the structure constants [9].

The self-energy is calculated by using $\epsilon_{\mathbf{k}n}$, $v_{ij}(\mathbf{k})$ and $\langle\psi_{\mathbf{q}n}|\psi_{\mathbf{q}-\mathbf{k}n'}\tilde{M}_i^{\mathbf{k}}\rangle$. The diagonal part of Σ_{x} is given by

$$\begin{aligned}&\langle\psi_{\mathbf{q}n}|\Sigma_{\mathrm{x}}|\psi_{\mathbf{q}n}\rangle\\ &= -\sum_{\mathbf{k}}^{\mathrm{BZ}}\sum_{ij}\sum_{n'}^{\mathrm{occ.}}\langle\psi_{\mathbf{q}n}|\psi_{\mathbf{q}-\mathbf{k}n'}\tilde{M}_i^{\mathbf{k}}\rangle v_{ij}(\mathbf{k})\langle\tilde{M}_j^{\mathbf{k}}\psi_{\mathbf{q}-\mathbf{k}n'}|\psi_{\mathbf{q}n}\rangle.\end{aligned} \tag{12}$$

The non-interacting polarization function D is expanded in the same manner as Eq.(11):

$$\begin{aligned}&D_{ij}(\mathbf{q},\omega)\\ &= \sum_{\mathbf{k}}^{\mathrm{BZ}}\sum_{n}^{\mathrm{occ.}}\sum_{n'}^{\mathrm{unocc.}}\langle M_i^{\mathbf{q}}\psi_{\mathbf{k}n}|\psi_{\mathbf{k}+\mathbf{q}n'}\rangle\langle\psi_{\mathbf{k}+\mathbf{q}n'}|\psi_{\mathbf{k}n}M_j^{\mathbf{q}}\rangle\\ &\quad\times\left[\frac{1}{\omega-\epsilon_{\mathbf{k}+\mathbf{q}n'}+\epsilon_{\mathbf{k}n}+i\delta}-\frac{1}{\omega+\epsilon_{\mathbf{k}+\mathbf{q}n'}-\epsilon_{\mathbf{k}n}-i\delta}\right].\end{aligned} \tag{13}$$

We use the tetrahedron method for the Brillouin zone (BZ) summation in Eq.(13) following Ref.[10]. The screened Coulomb interaction is given by $W = (1 - vD)^{-1}v$ in the random-phase approximation (RPA). W is also represented by the mixed basis.

The correlation part of the self-energy is calculated as

$$\begin{aligned}&\langle\psi_{\mathbf{q}n}|\Sigma_{\mathrm{c}}(\omega)|\psi_{\mathbf{q}n}\rangle\\ &= \sum_{\mathbf{k}}^{\mathrm{BZ}}\sum_{n'}^{\mathrm{All}}\sum_{ij}\langle\psi_{\mathbf{q}n}|\psi_{\mathbf{q}-\mathbf{k}n'}\tilde{M}_i^{\mathbf{k}}\rangle\langle\tilde{M}_j^{\mathbf{k}}\psi_{\mathbf{q}-\mathbf{k}n'}|\psi_{\mathbf{q}n}\rangle\\ &\quad\times\frac{i}{2\pi}\int_{-\infty}^{\infty}\frac{W_{ij}^{\mathrm{c}}(\mathbf{k},\omega')}{\omega+\omega'-\epsilon_{\mathbf{q}-\mathbf{k}n'}\pm i\delta}d\omega',\end{aligned} \tag{14}$$

where $-i\delta$ is taken for the occupied states and $+i\delta$ for the unoccupied states. We perform the frequency integration in Eq.(14) with a method devised by Aryasetiawan [3].

The evaluation of the exchange self-energy must be carried out carefully since the Coulomb interaction $v_{ij}(\mathbf{k})$ shows a singular behavior $v_{ij}(\mathbf{k}) \propto \frac{U_i^{0*}(\mathbf{k})U_j^0(\mathbf{k})}{|\mathbf{k}|^2}$ as $\mathbf{k} \to 0$, where $U_j^0(\mathbf{k})$ denotes the corresponding normalized eigenfunction. The singularity also exists in W. To handle the singular behavior, we use the offset Γ-point method [9], which is essentially equivalent to the method to integrate the divergent part analytically [2].

The QP energies are calculated with including the core contributions through the following equation,

$$\begin{aligned}E_{\mathbf{k}n} &= \epsilon_{\mathbf{k}n} + Z_{\mathbf{k}n}[\ \langle\psi_{\mathbf{k}n}|\Sigma_{\mathrm{x}}^{\mathrm{core1}} + \Sigma_{\mathrm{xc}}^{\mathrm{core2+valence}}|\psi_{\mathbf{k}n}\rangle\\ &\quad - \langle\psi_{\mathbf{k}n}|V_{\mathrm{xc}}^{\mathrm{LDA}}(n_{\mathrm{total}})|\psi_{\mathbf{k}n}\rangle\ ],\end{aligned} \tag{15}$$

where we divide the core states into two groups: core1 is the deep core state, which affects the QP energies only through Σ_{x}, and core2 is the relatively shallow core, which is treated on the same footing as the valence electrons.

III. RESULTS FOR ZINC OXIDE

We first describe the LDA calculation performed using the full-potential LAPW method. The local exchange-correlation functional of Vosko, Wilk and Nusair [11] is employed. The space group of wurtzite ZnO is $P6_3mc$. The lattice constant and the MT-sphere radii are given in Table I. The angular-momentum in the spherical-wave expansion is truncated at $l_{\max} = 6$ and $l_{\max} = 4$ for the potential and the wavefunction, respectively. This $l_{\max} = 4$ value is rather small, which gives errors compared with more accurate calculations with $l_{\max} = 7$, but the differences of them are within 0.02 eV for the LDA band gap. The energy cut-off of the IPW is 16Ry for the wavefunction. We take 1152 k-points in the first Brillouin zone (BZ). The Zn $(3d)^{10}(4s)^2$ and O $(2s)^2(2p)^4$ electrons are treated as valence electrons.

The GW calculation is performed with 32 k-points in the BZ. The energy cut-off of the IPW is 10 Ry for the Coulomb matrix. We treat 18 occupied bands and take into account 100 unoccupied bands. When producing the product basis, we ignore the product functions including $\phi_{al\beta=2}$ because the terms make small contributions. The Zn $3p$ states, which is relatively shallow in the core states, are chosen to be core2 electrons, i.e., the Zn $3p$ states are treated on the same footing as valence states and taken into account for the calculation of the correlation part of the self-energy. All the core and valence electrons are included into the calculation of the exchange part of the self-energy. In Sec. III C, we check the convergence of the QP energies in k-points, plane waves, unoccupied states, and product functions.

A. LDA

Unless otherwise stated, results in this section refer to the LAPW method. The LDA band structure for ZnO is shown in Fig. 1 and the density of states (DOS) is shown in Fig. 2. All energies are given with respect to the top of the valence band. Around −17 eV, we obtain two bands originating from the O $2s$ states. The narrow bands between −6 and −4 eV consist mainly of the Zn $3d$ orbitals, and the moderately dispersive bands from −4 to 0 eV consist mainly of the O $2p$ orbitals. Fig. 2 shows significant p-d hybridization. The Zn $3d$-derived bands are split into two groups, leading to a double-peak structure in the DOS. The lower peak is characterized by the strong p-d hybridization. The sharp upper peak between −4.8 and −4.2 eV has strong Zn $3d$ character and the hybridization with the O $2p$ states is very small. The band gap opens between the 18th and 19th bands and the fundamental gap of 0.77 eV is located at the Γ point. The lowest two conduction bands consist mainly of the Zn $4s$ orbitals. The energy levels at the Γ point computed by the LAPW method are shown in Table II. Also shown are the levels computed by the LMTO method. Agreement is excellent; the bandgaps are nearly identical and the bands agree to within 0.1 eV over the entire valence bands. A further check was made using an entirely different kind of LMTO method [13], and similar agreement was found.

The band dispersion is similar to the result of the norm-conserving pseudopotential method by Schröer, Krüger and Pollmann [14]. One important discrepancy is the magnitude of the band gap: their fundamental gap is only 0.23 eV. Other reported LDA gaps are 0.93 eV calculated with the full-potential LAPW method [15] and 1.15 eV within the LMTO-ASA method [16].

B. GWA

The *GW* band structure computed with LAPW input is shown in Fig. 3 together with the LDA band structure. In the figure, all energies are given with respect to the top of the valence band (the valence-band top in the GWA was shifted up 0.49 eV relative to the LDA). We also show the LDA, *GW* and HFA energies at the Γ point in Table II. The first and second bands are the O $2s$ bands, the 3-12th are mostly Zn $3d$ character, bands 13-18 are of mostly O $2p$ character, and bands 19-20 the Zn $4s$ conduction bands. Because the Zn $3d$ bands and the O $2p$ bands overlap in energy, the characterization of the band is more complicated: e.g., at the Γ point, the LDA 8th state has an O $2p$ character, while the 13th state has a Zn $3d$ character.

The self-energy correction is sensitive to the character of the band, as seen from Table II. The lowest O $2s$ bands are shifted by ~ -1 eV; the Zn $3d$ bands by ~ -1 eV; the conduction Zn $4s$ bands by $\sim +2$ eV. The Zn $3d$ bandwidth shrinks, while the O $2p$ bandwidth and the Zn $4s$ bandwidth are enhanced. The O $2s$ bandwidth does not change.

The LAPW gaps are 0.77 eV, 2.44 eV and 11.39 eV in the LDA, GWA and HFA, respectively, as Table II shows, for the 32 k-point mesh employed. The LMTO results are very similar. The experimental gap is 3.44 eV [16]. The large HFA gap reflects the neglect of screening the exchange while the LDA gap is too small largely because it neglects the nonlocality in the (screened) exchange altogether [17]. The *GW* gap is closer to the experiment but still smaller by $\sim$1 eV than the experimental gap. Previously reported *GW* gaps are somewhat larger. Using a model *GW* approach, Massidda et al. found a gap of 4.23 eV [15] and Oshikiri et al. found a gap of 4.28 eV [16] using an all-electron approach within the atomic spheres approximation. The major part of the error in our gap energy is thought to be derived from the overestimate of the dielectric function, originating from underestimated LDA gap used to generate it. We have found previously [5] that *GW* gaps are systematically underestimated in semiconductors, with the error increasing with ionicity. Using an all-electron *GW* implementation within the PAW method (albeit including valence-only electrons in the *GW* calculation), Arnaud and Alouani [18] have also noted a tendency for the *GW* band gaps to be smaller than the experimental ones. For example, for Si, they find a gap of 1.00 eV. Using a fully converged 512 k-point mesh, our LAPW-*GW* gap is 0.88 eV and our LMTO-*GW* gap is 0.89 eV. Wei Ku [19] has recently reported the LAPW-*GW* gap of 0.85 eV using a 512 k-point mesh.

The centers of the O $2s$ band and the Zn $3d$ band are -20.7 eV [20] and -8.81 eV [21], respectively, in experiment. Table II shows that those *GW* bands are located higher by about 2 eV than the experimental positions. The HFA result is rather closer to the experiment. In our calculation, the dielectric function is overestimated for the reasons listed below. (1) In the RPA, the electric attractive force is neglected between excited electron and hole; there is no restoring force for the polarization, leading to the overestimation of the polarization function. (2) The LDA band structure has a much smaller band gap than the experimental one. The electron-hole pair excitation energy is smaller than the real system. Since we use the LDA band structure to calculate the polarization function, we overestimate it. (3) The Zn $3d$ and O $2p$ bands are well separated in experiment, while they partly overlap in the LDA. The hybridization between the Zn $3d$ orbital and the O $2p$ orbital is overestimated. The hybridization between the Zn $4s$ orbital and the O $2p$ orbital is also overestimated because of the smaller bandgap in the LDA. This property of the LDA wavefunction makes the charge transfer between Zn and O, leading to the overestimation of the polarization function. All those procedures of our calculation causes the overestimation of the dielectric function, and, therefore, the screened Coulomb interaction, W. In order to improve our calculation in the latter two points of (2) and (3), we need to perform a self-consistent calculation, that is, to use the QP energies and wavefunctions to calculate the screened Coulomb interaction W.

In Table III, we show the real part of Σ at the Γ point. In the table, we take notations, $\Sigma^{\rm GWA}_{\mathbf{k}n} \equiv \langle\psi_{\mathbf{k}n}|\Sigma(\epsilon_{\mathbf{k}n})|\psi_{\mathbf{k}n}\rangle$ and $\Sigma^{\rm LDA}_{\mathbf{k}n} \equiv \langle\psi_{\mathbf{k}n}|V^{\rm LDA}_{\rm xc}|\psi_{\mathbf{k}n}\rangle$; the self-energy corrections are given by $Z_{\mathbf{k}n}[\Sigma^{\rm GWA}_{\mathbf{k}n} - \Sigma^{\rm LDA}_{\mathbf{k}n}]$. The normalization factor $Z_{\mathbf{k}n}$ is between 0.66 and 0.81, which is comparable to simple metals or semiconductors. As noted before, the self-energy corrections are negative for the valence bands and positive for the conduction bands and are larger for the localized states. Table IV shows the decomposition of $\Sigma^{\rm GWA}_{\mathbf{k}n}$ at the Γ point to the core-exchange part $\Sigma^{\rm xcore1}_{\mathbf{k}n}$, the exchange part $\Sigma^{\rm x}_{\mathbf{k}n}$, and the correlation part $\Sigma^{\rm c}_{\mathbf{k}n}$. The contributions of the core2 electrons are included in $\Sigma^{\rm x}_{\mathbf{k}n}$ and $\Sigma^{\rm c}_{\mathbf{k}n}$. The exchange part $\Sigma^{\rm x}_{\mathbf{k}n}$ has a large discontinuity across the Fermi level, leading to the wide gap in the HFA. The correlation part $\Sigma^{\rm c}_{\mathbf{k}n}$ are positive for the valence bands and negative for the conduction bands, leading to the reduction of the bandgap from the HFA value.

C. Convergence check

The *GW* band structures described in Sec.III B have been calculated using 32 k-points in the BZ, an IPW energy cutoff of 10 Ry for the Coulomb matrix, 100 unoccupied states, and neglecting products including $\phi_{al\beta=2}$. To check the convergence of the QP energies, we have performed *GW* calculations with some different conditions. The conditions we have used are 64 k-points 144 k-points, the energy cut-off of 16 Ry for the IPW, or 200 unoccupied states. The results are shown in Table V-VII, compared to the result in Sec.III B. In any case, the errors are within 0.1 eV. We have also performed the calculation with the products including $\phi_{al\beta=2}$ for Zn. The improvement is quite small, within 0.005 eV. Our *GW* result thus shows good convergence; especially, a small number of IPW is enough to achieve a good result.

We have checked the influence of the Zn 3p core states. In Sec.III B, we have treated the states as core2, i.e. they treated on the same footing as valence states. Now, we treat the Zn 3p states as core1 (and include the products with $\phi_{al\beta=2}$ for Zn). The fundamental gap becomes 2.47 eV and the Zn 3d bands are shifted lower by $\sim$ 0.1 eV. The effect of the Zn 3p electrons on the valence band through the correlation term in the self-energy is about 0.1 eV.

IV. SUMMARY

We have presented a procedure for calculating the self-energy in the GWA with the mixed-basis expansion based on the full-potential LAPW and LMTO methods, and have applied the all-electron *GW* calculation to wurtzite ZnO. The mixed-basis method works well for this system which has both extended states and localized states; the *GW* calculation has a good convergence in various parameters, and can be performed on a workstation-level computer.

The *GW* bandgap of ZnO is smaller than experiment by ~ 1 eV. The self-energy correction is orbital dependent and the localized O 2s and Zn 3d states are lowered by $\sim$ 1eV relative to the LDA values, while still higher than experiment. The *GW* calculation overestimates the screening effect for localized states such as the Zn 3d states, because of the RPA and the LDA band structure. These errors are apparently systematic in zincblende semiconductors [5]. We have indicated that a self-consistent calculation can improve the result.

For a four-atom system having localized 3d orbitals such as wurtzite ZnO, we can complete the *GW* calculation with 32 k-points in the BZ within three days by using a DEC alpha 21264 667MHz workstation. Our *GW* code is available in a web site. The address is http://al1.phys.sci.osaka-u.ac.jp

Acknowledgments

We would like to thank Dr. Ferdi Aryasetiawan for many helpful discussions. This work is supported by the Research Fellowships of the Japan Society for the Promotion of Science for Young Scientists. This work is also supported by a Grant-in-Aid for "Research for the Future" Program from the Promotion of Science. MvS was supported by the Office of Basic Energy Sciences, under contract no. DE-AC04-94AL85000.

---

[1] L. Hedin, Phys. Rev. **139**, A796 (1965); L. Hedin and S. Lundqvist, in *Solid State Physics*, edited by F. Seitz, and D. Turnbull, and H. Ehrenreich (Academic, New York, 1969), Vol. 23, p. 1.

[2] M. S. Hybertsen and S. G. Louie, Phys. Rev. B **34**, 5390 (1986).

[3] F. Aryasetiawan in *Strong Coulomb Correlations in Electronic Structure Calculations*, edited by V. I. Anisimov (Gordon and Breach Science Publishers, 2000).

[4] T. Takeda and J. Kübler, J. Phys. F **9**, 661 (1979); H. J. F. Jansen and A. J. Freeman, Phys. Rev. B **30**, 561 (1984).

[5] T. Kotani and M. van Schilfgaarde, to appear in Solid State Communications.

[6] M. Methfessel, M. van Schilfgaarde, and R. A. Casali, *Electronic Structure and Physical Properties of Solids: The Uses of the LMTO Method*, *Lecture Notes in Physics*, **535**. H. Dreysse, ed. (Springer-Verlag, Berlin) 2000.

[7] F. Aryasetiawan and O. Gunnarsson, Phys. Rev. B **49**, 16214 (1994).

[8] M. Joseph, H. Tabata and T. Kawai, Jpn. J. Appl. Phys. **38** L1205 (1999).

[9] T. Kotani, M. van Schilfgaarde, M. Usuda and N. Hamada, (in preparation).

[10] J. Rath and A. J. Freeman, Phys. Rev. B **11**, 2109 (1975).

[11] S. H. Vosko, L. Wilk, and M. Nusair, Can. J. Phys. **58**, 1200 (1980).

[12] H. Schulz and K. H. Theimann, Sol. St. Comm. **32**, 783 (1979).

[13] M. Methfessel, Phys. Rev. B **38** 1537 (1988).

[14] P. Schröer, P. Krüger and J. Pollmann, Phys. Rev. B **47**, 6971 (1993).

[15] S. Massidda, R. Resta, M. Posternak and A. Baldereschi, Phys. Rev. B **52**, R16977 (1995).

[16] M. Oshikiri and F. Aryasetiawan, J. Phys. Soc. Jpn. 69 2123 (2000).

[17] E. M. Maksimov, I. I. Mazin, S. Yu. Savrasov and Yu. A. Uspenski, J. Phys. Condens. Matter, **1** 2493 (1989).

[18] B. Arnaud and M. Alouani, Phys. Rev. B **62**, 4464 (2000).

[19] Wei Ku and Adolfo Eguilez, preprint.

[20] L. Ley, R. A. Pollak, F. R. McFeely, S. P. Kowalczyk and D. A. Shirley, Phys. Rev. B **9**, 600 (1974).

[21] This value is taken from Ref.[20]. On the other hands, different values for the center of the Zn 3d position are also reported; -8.6 eV by C. J. Vesely and D. W. Langer,

Phys. Rev. B **4**, 451 (1971); −7.5 eV by R. A. Powell, W. E. Spicer and J. C. McMenamin, Phys. Rev. B **6**, 3056 (1972).

TABLE I: Crystal structure and MT radii for wurtzite ZnO. Atomic positions are $(\frac{1}{3},\frac{2}{3},0)$ and $(\frac{2}{3},\frac{1}{3},\frac{1}{2})$ for Zn, and $(\frac{1}{3},\frac{2}{3},u)$ and $(\frac{2}{3},\frac{1}{3},u+\frac{1}{2})$ for O. We use experimental values of a and c given in Ref. [12], while the u-parameter of O is estimated within the LDA separately with the LAPW and LMTO calculations. The change in eigenvalues computed with the two different values of u is small. In some of the LMTO calculations, an empty sphere was added to enlarge the basis set.

	LAPW	LMTO
a [Å]	3.253[a]	3.253[a]
c/a	1.6025[a]	1.6025[a]
u	0.3817	0.3825
Zn radius [a.u.]	2.0	2.13
O radius [a.u.]	1.4	1.70
Es radius [a.u.]		2.04

[a] Reference [12].

TABLE II: The LDA, GW and HFA energies (in eV) at $\mathbf{k}=(0,0,0)$. All energies are given with respect to the top of the valence band. The LAPW-GW and LMTO-GW results use 32 and 216 k-points, respectively. As shown in Tables V, VI and VII, the LAPW-GW fundamental gap would be 0.05 to 0.1 eV smaller if the combined effect of complete convergence in k-points, IPW and number of unoccupied states were taken into account.

	LDA		GWA		HFA
Band n	LAPW	LMTO	LAPW	LMTO	LAPW
1	−17.84	−17.74	−18.56	−18.37	−23.17
2	−17.06	−16.97	−17.78	−17.67	−22.42
3,4	−5.80	−5.77	−6.62	−6.51	−9.95
5	−5.74	−5.70	−6.58	−6.49	−9.99
6,7	−5.62	−5.59	−6.46	−6.34	−9.80
8	−5.53	−5.61	−5.65	−5.59	−5.58
9,10	−4.70	−4.63	−5.90	−5.82	−9.87
11,12	−4.48	−4.42	−5.68	−5.61	−9.75
13	−4.19	−4.12	−5.20	−5.13	−8.92
14,15	−0.74	−0.79	−0.84	−0.87	−0.89
16	−0.10	−0.09	−0.08	−0.03	−0.00
17,18	0	0	0	0	0
19	0.77	0.78	2.44	2.44	11.39
20	5.13	5.12	7.19	7.25	17.13

TABLE III: GW self-energies $\Sigma_{\mathbf{k}n}^{\mathrm{GWA}}$ at $\mathbf{k} = (0, 0, 0)$, together with the LDA exchange-correlation term $\Sigma_{\mathbf{k}n}^{\mathrm{LDA}}$ and the renormalization factor $Z_{\mathbf{k}n}$. The corrections are given by $Z_{\mathbf{k}n}[\Sigma_{\mathbf{k}n}^{\mathrm{GWA}} - \Sigma_{\mathbf{k}n}^{\mathrm{LDA}}]$.

Band n	$\Sigma_{\mathbf{k}n}^{\mathrm{GWA}}$ [eV]	$\Sigma_{\mathbf{k}n}^{\mathrm{LDA}}$ [eV]	$Z_{\mathbf{k}n}$	Corrections [eV]
1	−22.09	−20.33	0.69	−1.22
2	−23.28	−21.45	0.66	−1.21
3,4	−35.25	−33.37	0.70	−1.32
5	−35.74	−33.83	0.70	−1.33
6,7	−35.74	−33.84	0.70	−1.33
8	−18.62	−17.74	0.70	−0.61
9,10	−41.70	−39.36	0.72	−1.69
11,12	−42.46	−40.11	0.72	−1.69
13	−40.66	−38.55	0.71	−1.50
14,15	−27.44	−26.65	0.75	−0.59
16	−27.93	−27.30	0.75	−0.47
17,18	−28.79	−28.13	0.75	−0.49
19	−12.87	−14.32	0.81	1.18
20	−12.45	−14.39	0.81	1.57

TABLE IV: Core-exchange part $\Sigma_{\mathbf{k}n}^{\mathrm{xcore1}}$, exchange part $\Sigma_{\mathbf{k}n}^{\mathrm{x}}$ and correlation part $\Sigma_{\mathbf{k}n}^{\mathrm{c}}$ of the GW self-energy at $\mathbf{k} = (0, 0, 0)$. The contributions of the core2 electrons are included in $\Sigma_{\mathbf{k}n}^{\mathrm{x}}$ and $\Sigma_{\mathbf{k}n}^{\mathrm{c}}$.

Band n	$\Sigma_{\mathbf{k}n}^{\mathrm{xcore1}}$ [eV]	$\Sigma_{\mathbf{k}n}^{\mathrm{x}}$ [eV]	$\Sigma_{\mathbf{k}n}^{\mathrm{c}}$ [eV]
1	−1.85	−29.84	9.60
2	−2.02	−30.81	9.55
3,4	−5.04	−38.51	8.29
5	−5.17	−38.93	8.36
6,7	−5.18	−38.87	8.31
8	−1.24	−22.57	5.20
9,10	−6.83	−43.73	8.85
11,12	−7.01	−44.39	8.95
13	−6.55	−42.75	8.65
14,15	−2.85	−29.97	5.39
16	−2.92	−30.31	5.30
17,18	−3.14	−31.02	5.37
19	−1.45	−8.27	−3.15
20	−1.44	−6.97	−4.04

TABLE V: Dependence on the QP energies on the number of k-points, for representative states at the Γ point. The calculation with 32 k points is the same one in Table II. The LMTO method was used to compute QP energies for finer meshes, up to 216 k-points (6×6×6 mesh). The LMTO-GW gap changed by −0.1 eV going from 64 to 216 k-points; assuming the same convergence in k-points within the LAPW method, we estimate the converged LAPW-GW fundamental gap to be 2.32 eV, keeping all other parameters fixed. The LAPW-GW and LMTO-GW energies agree with each other to within 0.1 eV, with the error approximately tracking differences in the LDA eigenvalues.

Band n	144 $\mathbf{k}$	64 $\mathbf{k}$	32 $\mathbf{k}$
1	−18.51	−18.54	−18.56
3	−6.60	−6.60	−6.62
8	−5.64	−5.62	−5.65
14	−0.84	−0.83	−0.84
18	0	0	0
19	2.35	2.42	2.44

TABLE VI: Dependence of the QP energies on the number of IPW used to make the the Coulomb matrix, for representative states at the Γ point. Data with the 10 Ry cutoff is the same as in Table II.

Band n	16 Ry	10 Ry
1	−18.55	−18.56
3	−6.59	−6.62
8	−5.64	−5.65
14	−0.84	−0.84
18	0	0
19	2.47	2.44

TABLE VII: Dependence of the QP energies on the number of the unoccupied states, for representative states at the Γ point. The calculation with 100 unoccupied states is the same as in Table II.

Band n	200 unocc.	100 unocc.
1	−18.56	−18.56
3	−6.54	−6.62
8	−5.62	−5.65
14	−0.83	−0.84
18	0	0
19	2.45	2.44

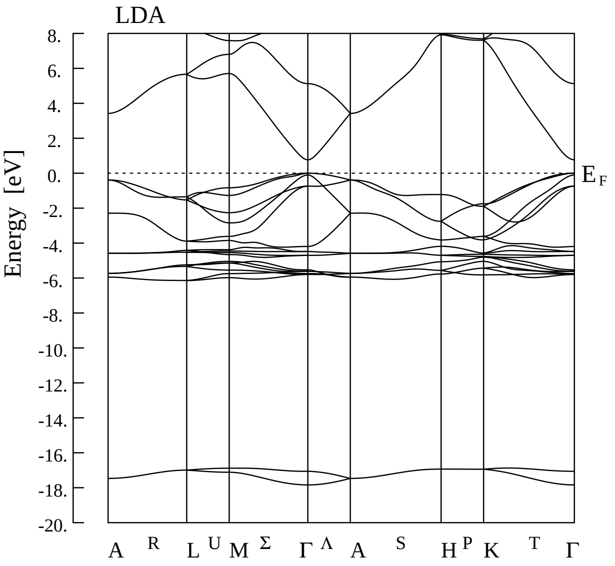

FIG. 1: LDA band structure in wurtzite ZnO.

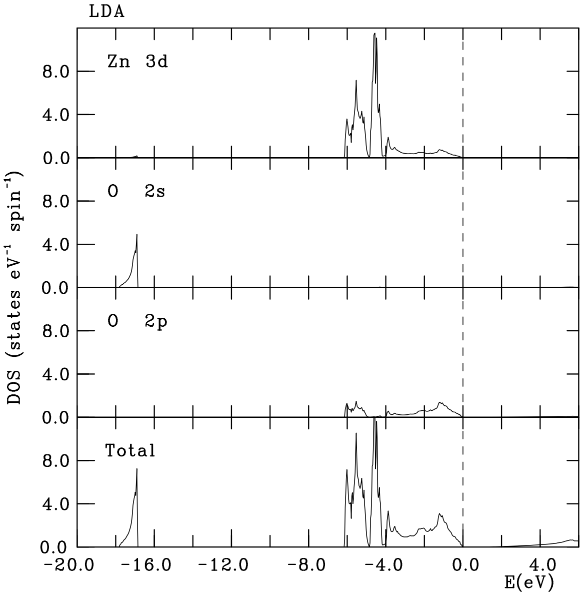

FIG. 2: Density of states in wurtzite ZnO.

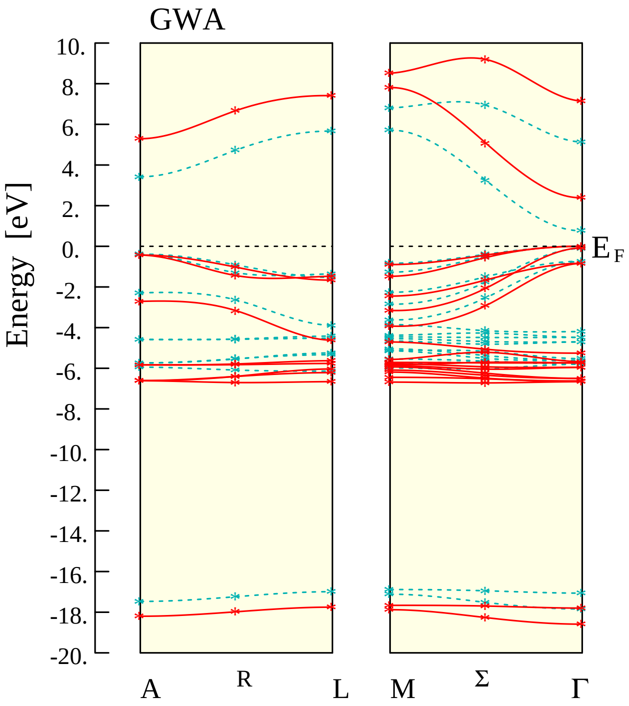

FIG. 3: The *GW* band structure (solid lines) and the LDA band structure (dashed lines) for wurtzite ZnO. The self-energy corrections are calculated at the points marked '$*$'.